Published in final edited form as:

J Proteome Res. 2016 May 06; 15(5): 1702–1716. doi:10.1021/acs.jproteome.6b00137.

Large-Scale, Ion-Current-Based Proteomic Investigation of the Rat Striatal Proteome in a Model of Short- and Long-Term Cocaine Withdrawal

Shichen Shen[2,3,#], **Xiaosheng Jiang**[1,2,#], **Jun Li**[1,2,#], **Robert M. Straubinger**[1], **Mauricio Suarez**[4,5], **Chengjian Tu**[2,3], **Xiaotao Duan**[6], **Alexis C. Thompson**[4,5,*], and **Jun Qu**[1,2,*]

[1]Department of Pharmaceutical Sciences, SUNY at Buffalo

[2]New York State Center of Excellence in Bioinformatics & Life Sciences, Buffalo, NY

[3]Department of Biochemistry, School of Medicine and Biomedical Sciences, SUNY at Buffalo

[4]Department of Psychology, SUNY at Buffalo

[5]Research Institute on Addictions, SUNY at Buffalo

[6]State Key Laboratory of Proteomics, Beijing Proteome Research Center, Beijing Institute of Radiation Medicine

Abstract

Given the tremendous detriments of cocaine dependence, effective diagnosis and patient stratification are critical for successful intervention, yet difficult to achieve due to the largely unknown molecular mechanisms involved. To obtain new insights into cocaine dependence and withdrawal, we employed a reproducible, reliable and large-scale proteomics approach to investigate the striatal proteomes of rats (n=40, 10 per group) subjected to chronic cocaine exposure followed by either short-(WD1) or long-(WD22) term withdrawal. By implementing a surfactant-aided precipitation/on-pellet digestion procedure, a reproducible and sensitive nanoLC-Orbitrap MS analysis, and an optimized ion-current-based MS1 quantification pipeline, >2,000 non-redundant proteins were quantified confidently without missing data in any replicate. Although cocaine was cleared from the body, 129/37 altered proteins were observed in WD1/WD22 that are implicated in several biological processes related closely to drug-induced neuroplasticity. Although many of these changes recapitulate the findings from independent studies reported over the last two decades, some novel insights were obtained and further validated by immunoassays. For example, significantly elevated striatal PKC activity persisted over the 22-day cocaine withdrawal. Cofilin-1 activity was up-regulated in WD1 and down-regulated in WD22. These discoveries suggest potentially distinct structural plasticity after short- and long-term cocaine withdrawal. In addition, this study provides compelling evidence that blood vessel narrowing, a long-known effect of cocaine use, occurred after long-term- but not short-term

[*]Corresponding Authors: Alexis C. Thompson, Ph.D, 357 Research Institute on Addictions, State University of New York at Buffalo, Buffalo, NY 14203, Phone: (716)887-2243, athompso@ria.buffalo.edu. Jun Qu, PhD, Department of Pharmaceutical Sciences, 318 Kapoor Hall, State University of New York at Buffalo, Buffalo, NY 14214, Phone: (716)881-7513, junqu@buffalo.edu.
[#]Authors contribute equally.

SUPPORTING INFORMATION AVAILABLE

These materials are available free of charge via the Internet at http://pubs.acs.org

withdrawal. In summary, this work developed a well-optimized paradigm for ion-current-based quantitative proteomics in brain tissues, and obtained novel insights into molecular alterations in the striatum following cocaine exposure and withdrawal.

Graphic Abstract

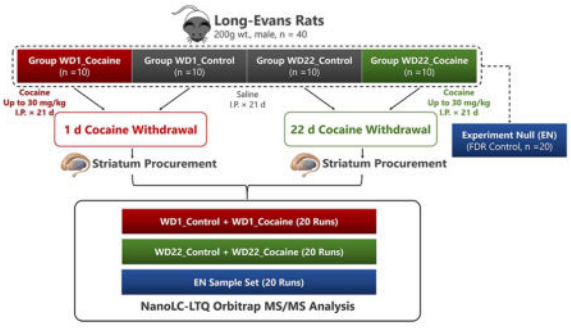

Keywords

Bottom-up Proteomics; Ion-Current-Based; Neuroplasticity; Cocaine Dependence; Cocaine Withdrawal

INTRODUCTION

Cocaine dependence is characterized by a maladaptive pattern of behaviors in which cocaine use is compulsive, and the psychological, social, and physical functioning of the individual is severely compromised[1]. Individuals with cocaine dependence usually suffer social incompetence (e.g. relationship failures, occupational inability, violation of legislation), and are at high risk of developing a number of fatal cardiovascular, pulmonary and immunological complications[2–4]. There are few effective pharmacotherapies against cocaine dependence, because of its complicated behavioral manifestations and poorly-understood changes in molecular pathways[5]. Accurate diagnosis of cocaine dependence is critical but difficult to perform, because few specific biomarkers have been developed[6].

In the United States, lifetime prevalence of cocaine use is about 25 million[1], with an estimation that as many as 17–20% of cocaine users will eventually develop cocaine dependence[7]. The mechanisms underlying the progression from occasional cocaine use to cocaine dependence are still insufficiently understood. One major hypothesis is that drug-induced neuroplasticity and its interaction with individual differences and experiential factors is an important contributor[8]. Several studies in rodent models have demonstrated that neuroplasticity is manipulated by cocaine exposure, and that experimentally regulating neuroplasticity would alter or possibly eliminate the dependence-like symptoms induced by chronic cocaine exposure[9, 10]. These findings suggest the role that neuroplasticity plays in the development of cocaine dependence, but greater insight into the molecular basis of such neuroplasticity is required to support this hypothesis.

Bouts of withdrawal (or abstinence) varying in length and context (e.g. with or without continued drug-cue exposure) are a common experiential feature shaping the behavioral adaptations underlying cocaine dependence and vulnerability to relapse. Elucidation of the molecular alterations occurring during withdrawal, and correlation of these changes with the lengths of withdrawal, have been a principal research focus over the last two decades, in the effort to understand cocaine dependence in general and to identify effective treatment strategies in specific[11]. Typically, hypothesis-driven strategies have been utilized to characterize the molecular and cellular adaptations associated with cocaine dependent behavior. However, the behavioral manifestations of cocaine dependence originate from an ensemble of numerous changes in molecules and their corresponding signaling pathways. Therefore, unbiased discovery-based approaches, such as proteomic profiling, hold the potential to provide not only unprecedented proteome-wide details of changes in proteins potentially involved in the etiology of drug addiction, but also for the identification of critical protein biomarkers that may facilitate the clinical stratification of individuals having a history of cocaine use[12]. However, this task is technically challenging to accomplish for several reasons.

First, given that behavioral manifestations of cocaine dependence are determined by numerous factors, the molecular presentation are guaranteed vary among different individuals. Therefore, inclusion of a large number of biological replicates (e.g. 10 animals per group) is desirable to enhance the quantitative reliability and statistical power of the results, and to alleviate the false-positive discovery of protein alterations that arise from biological variation. Great progress in the proteomic investigation of drug addiction has been made using either 2D-DIGE[13, 14] or isotope-labeling approaches[15]. However, when quantitative values for individual biological replicates are desired among a cohort with large sample size, as in this study and many biomedical investigations, these techniques may still fall short due to the relatively limited multiplexing capacity.

Second, in order to reveal comprehensively the underlying mechanisms of cocaine dependence, an approach for accurate quantification of striatal proteins, especially low-abundance regulatory proteins, is essential. However, this is difficult to achieve because of the high complexity and wide dynamic range of protein abundance in brain tissues[16]. Advances such as pre-fractionation by multi-dimensional chromatography has improved proteomic coverage remarkably [17, 18], but such strategies are impractical for the analysis of the larger numbers of biological replicates employed to improve quantitative reliability in the current study. Furthermore, the brain proteome contains a large proportion of membrane-bound proteins, which are difficult to extract and analyze in a quantitative fashion using conventional proteomic approaches [19].

Finally, the extent of protein changes during cocaine withdrawal are likely to be subtle, even after just 24 hr of withdrawal, a time at which most bioactive metabolites of cocaine are eliminated biologically [20]. As a result, accurate quantification of these changes can be difficult technically and liable to variations. A highly accurate and precise strategy is required so that confident quantification of proteins having the anticipated low-fold changes can be achieved. The determination of proteins that are altered significantly, but relatively low in fold change, is particularly liable to false-positive discoveries, which arise from both

biological and technical variation[21, 22]. False-positive discoveries convey misleading biological information and should be minimized. However, the false discovery of altered proteins remains underrepresented for MS-based quantitative proteomics[23].

Here we address these challenges by employing a comprehensive, reproducible, and well-controlled proteomics strategy, enabling 1) reliable proteomic comparisons involving a large number of biological replicates; 2) comprehensive characterization of the striatal proteome; 3) accurate determination of low-magnitude protein changes with effective control of the false-positive biomarker discovery rate. This strategy includes an efficient sample preparation procedure that provides high and quantitative peptide recovery, an extensive and reproducible nanoLC-Orbitrap MS/MS analysis, and an experimental approach to select the optimal thresholds for determining significantly altered proteins. Using this strategy, we conducted a relatively large-scale investigation (n = 40 subjects in total) of the effects of cocaine withdrawal on the rat striatal proteome, a critical region of the basal ganglia system. The striatum was chosen as the target for investigation because it is likely to be closely associated in the aforementioned behavioral manifestations induced by cocaine exposure. Previous studies have demonstrated the enrichment of cocaine in the striatal area, suggesting that this region may be affected substantially by cocaine use[24]. The striatum also plays pivotal roles in the integration of cognitive learning and addiction, thus making it highly relevant to cocaine dependence[25]. We hypothesize that withdrawal from cocaine induces changes of proteomic patterns in the striatum, potentially accounting for the behavioral characteristics related to cocaine dependence. Moreover, because neurochemical changes described to date are fluid over the first month of withdrawal, proteomic changes were expected to reflect the length of withdrawal. Therefore, two different withdrawal periods were investigated: after 21 days of chronic cocaine treatment, the animals were subjected to a c short (1 day) or long (22 days) period of withdrawal. The selection of time points for sample collection was driven by the availability of the large body of neurochemical, biochemical, and behavioral literature that pertains to the first 3 weeks of withdrawal[26]. Significantly altered proteins and biological networks of interests were examined further by immunoassays.

MATERIALS & METHODS

Animal Experiments

Forty male Long-Evans (hooded) rats (Harlan Sprague Dawley, Indianapolis, IN) of approximately 200–225 g were housed as weight-matched pairs (+/− 5 g at initial pairing) in clear, free standing, polycarbonate cages (46 × 25 × 21 cm) filled with 1–2″ aspen hardwood shavings (Northeastern Products, New York, NY). Food (Teklad Rodent Diet 2018, Harlan Teklad, Madison, WI) and tap water were accessible *ad libitum*. The colony room was maintained under a 14:10 light: dark cycle (lights on at 0600 h, EST) at 22° ± 2 °C and 30–70% relative humidity. Rats were allowed 5–7 days to acclimate before cocaine administration began. All procedures were conducted in accordance with federal, state and institutional guidelines for the care and use of animal subjects and were approved by the University at Buffalo Institutional Animal Care and Use Committee. The animal

facilities were accredited by the Association for Assessment and Accreditation of Laboratory Animal Care, International.

Rats were administered cocaine or vehicle for 21 days and then sacrificed 1 d (WD1) or 22 d (WD22) after the last administration. All administrations were delivered in the home cage and co-housed pairs of rats received the same treatment. Cocaine was administered i.p. in the following escalating dose regimen: 5 mg/kg (day 1–2), 10 mg/kg (day 3–4), 15 mg/kg (day 5–6), 20 mg/kg (day 7–17), and 30 mg/kg (day 18–21) in a volume of 2 mL/kg. Control rats received physiological saline (vehicle) daily at 2 mL/kg. Doses were administered between 0700 and 2000 h EST in a random manner in order to avoid association of drug treatment with the time in a day, except on day 21, when injections were given between 1200 and 1400 h EST (the same time at which rats would be sacrificed).

Sample Procurement & Preparation

Rats (n=10 per group) were sacrificed on day 22, 24 h after the last cocaine injection (WD1) or at the same time on day 43 with an additional 22 days of cocaine withdrawal (WD22). Striatal tissue was procured by free-hand dissection after decapitation, following the procedures described by Chiu et al[27]. The tissues were rapidly frozen in liquid nitrogen and stored at −80 °C until analysis.

For protein extraction, the striatal tissue was thawed at room temperature and dissolved in 500 μL of ice-cold lysis buffer containing 50 mM Tris-FA, 150 mM NaCl, 0.5% sodium deoxycholate, 2% SDS, and 2% IGEPAL® CA-630 (pH 8.0; Sigma-Aldrich, St. Louis, MO). Protease inhibitor cocktail tablets and phosphatase inhibitor cocktail tablets (Roche Applied Science, Indianapolis, IN) were also added. Homogenization of the tissue/lysis buffer mixture was done by 5–10 cycles of homogenization (15,000 rpm, 5–10 s) and cooling (~20 s) cycles using a Polytron homogenizer (Kinematica AG, Switzerland). The samples were then sonicated until the liquid became clear, and allowed to settle on ice for ~30 min. After centrifugation at 20,000 g at 4 °C for 1 hr, the supernatants were carefully transferred to individual Eppendorf tubes, and the protein concentrations were determined using a bicinchoninic acid assay (BCA) kit (Pierce Biotechnology, Inc., Rockford, IL).

Surfactant-Aided Precipitation/On-Pellet Digestion (SOD)

For each sample, 100 μg of extracted proteins was used according to protein concentrations determined by BCA. Proteins were reduced and alkylated with 3 mM tris(2-carboxyl)phosphine (TCEP) and 20 mM iodoacetamide (IAM). Both steps were conducted with 30 min incubation in darkness at 37 °C with consistent oscillation in an Eppendorf Thermomixer (Eppendorf, Hauppauge, NY). Protein precipitation was performed afterward by stepwise addition of 9 volumes of ice-cold acetone and overnight incubation at −20 °C. The precipitated proteins were pelleted by centrifugation at 20,000 g at 4 °C for 30 min, and the supernatant portion containing undesirable components (e.g. detergents, phospholipids) was discarded. Protein pellets were then rinsed with 800 μL of ice-cold acetone/ddH_2O mixture (85/15, v/v %) and air-dried for ~5 min.

For the digestion step, protein pellets were suspended with 80 μL of Tris-FA buffer and briefly sonicated. Trypsin from porcine pancreas (Sigma-Aldrich, St. Louis, MO) was

dissolved in 80 μL of Tris-FA buffer to a concentration of 0.25 μg/μL, and digestion was performed in a two-step procedure: 1) digestion-aided pellet dissolution: trypsin at an enzyme/substrate ratio of 1:40 (w/w) was added to the protein pellets, and the mixture was incubated at 37 °C for 6 hr with constant vortexing in an Eppendorf Thermomixer; 2) complete cleavage: a second aliquot of same amount of trypsin was added to the re-dissolved and partially-cleaved proteins, and the mixture was incubated at 37 °C overnight (12–16 hr). Digestion was terminated by addition of 1μL formic acid (FA), followed by centrifugation at 20,000 g at 4 °C for 30 min to remove particulate impurities. The supernatants, containing tryptic peptides derived from 6 μg of protein, was analyzed by LC-MS.

Long-Gradient Nano RPLC-Mass Spectrometry

A uniquely designed and optimized LC-MS/MS strategy with high efficiency and reproducibility was employed to separate and analyze peptides converted from proteins extracts. The nano RPLC system consisted of a Spark Endurance autosampler (Emmen, Holland) and an ultrahigh pressure Eksigent (Dublin, CA) Nano-2D Ultra capillary/nano LC system. To achieve comprehensive separation of the complex peptide mixture, a nano LC/nanospray setup that featured low void volume and high chromatographic reproducibility was employed. Mobile phases A and B were 0.1% FA in 2% acetonitrile (ACN) and 0.1% FA in 88% ACN. Samples were loaded onto a large-ID trap (300 um ID × 1 cm, packed with Zorbax 3 m C18 material) with 1% B at a flow rate of 10 μl/min, and the trap was washed for 3 min before being brought in line with the nano LC flow path. The nano LC column was heated uniformly at 52 °C to improve chromatographic resolution and reproducibility. A series of nanoflow step gradients at a flow rate of 250 nL/min was utilized to back-flush the trapped samples onto the nano LC column (75 um ID × 100 cm, packed with Pepmap 3-m C18 material) for separation. A 7 hr shallow gradient was used to achieve extensive peptide separation. The optimized gradient profile was: 3 to 8% B over 15 min; 8 to 24% B over 215 min; 24 to 38% B over 115 min; 38 to 63% B over 55 min; 63 to 97% B in 5 min, and finally isocratic at 97% B for 15 min.

For peptide detection, an LTQ Orbitrap XL mass spectrometer (Thermo Fisher Scientific, San Jose, CA) was employed. Rinsing and conditioning of the nanospray needle was performed after every three runs by dripping 50% methanol on it, so that reproducibility of ionization efficiency could be maintained. The instrument was operated in the data-dependent product ion mode. One scan cycle consisted of an MS1 survey scan (*m/z* 310–2000) at a resolution of 60,000, followed by seven MS2 scans by CID activation mode to fragment the seven most abundant precursors in the survey scan. Because the use of high target value on Orbitrap allowed highly sensitive detection with little compromise of mass accuracy and resolution, the target value for MS1 was set to 8×10^6. Charge state screening was enabled to select precursor ions with 2–7 charges. Dynamic exclusion was enabled with the following settings: repeat count = 1; repeat duration = 30 s; exclusion list size = 500; and exclusion duration = 40 s. The activation time was 30 ms with an isolation width of 3 Da for ITMS; the normalized activation energy was 35%, and the activation q was 0.25. Ten samples from each group (WD1_Cocaine, WD1_Control, WD22_Cocaine, and WD22_Control) were analyzed in random order.

Protein Identification & Quantification

Individual LC-MS/MS raw files were imported into SEQUEST-embedded Proteome Discover (version 1.4.1.14, Thermo Scientific) and searched against the Rattus Norvegicus UniProt-Swissprot/TrEMBL protein database (release of Feb 2015) with 34,164 protein entries. The searching parameters included: 15 ppm tolerance for precursor ion mass, 1.0 Da tolerance for fragment ion mass, maximally two missed cleavages permitted for fully tryptic peptides, carbamidomethylation of cysteine as the fixed modification, and oxidation of methionine as the dynamic modification. Post identification processing, protein grouping, and false discovery rate (FDR) control were accomplished by Scaffold (v4.3.2, Proteome Software Inc.)[28] using a target-decoy search strategy with a concatenated database containing both forward and reverse sequences[29]. Corresponding filtering parameters included: 6 for minimal peptide length, 25 PPM for parent mass tolerance, 0.1 for DeltaCn, 1.3, 1.7, 2.3 and 2.7 Xcorr thresholds for singly-, doubly-, triply- and quadruply-charged ions.

Chromatographic alignment and global intensity-based MS1 feature detection/extraction were performed using SIEVE (v2.1.377, Thermo Scientific)[30]. The 3 primary steps included: 1) chromatographic alignment among LC-MS/MS runs by applying the ChromAlign algorithm; quality control of LC-MS/MS runs was achieved by monitoring and benchmarking the alignment scores and base-peak-ion current intensity. 2) determination of quantitative “frames” based on *m/z* and retention time in the aligned collective dataset; only frames with high-quality AUC data (e.g. signal-to-noise ratio >10) were selected, in order to achieve reliable quantification. 3) Calculation of peptide ion intensities for each frame. The resulting .sdb files were incorporated with spectrum reports exported from Scaffold with the MS2 fragmentation scans associated with each frame using R scripts. Another R package developed in-house was utilized for the normalization of ion current intensities for each protein (by quantile ion intensities among individual runs) and the aggregation of sum ion intensities from “frame” levels to protein levels. The calculation of the protein expression ratio, as well as the evaluation of statistical significance with Student’s *t* test between experimental and control groups, were also conducted to determine the significantly altered proteins. Quantification by spectral counting was also performed and compared with our ion-current-based method. Protein quantitative values (unique spectral counts) based on spectral-counting was obtained from Scaffold using the same identification parameters as described above.

Experimental FDR Estimation &Control for Altered Proteins

In order to estimate and control the false-positives in significantly altered proteins arising from technical variability, an experimental approach was devised. Small portions of protein mixtures from all control (no drug) samples (n = 10) were pooled, and twenty identical aliquots of the pooled samples (containing 100 μg of extracted proteins) were prepared as the Experimental Null (EN) sample set. From the EN sample set, 10 randomly picked samples were designated as EN_Control and the other 10 were designated as EN_Cocaine. Tryptic digestion and LC-MS/MS analyses of the EN sample set followed the same protocol as for the WD1 and WD22 sample sets.

Bioinformatics Analyses

Gene Ontology (Go) analysis was conducted using the Database for Annotation, Visualization and Integrated Discovery (DAVID) Bioinformatics Resources v6.7 (http://david.abcc.ncifcrf.gov)[31]. Biological processes and cellular components assigned by the tool were manually examined and regrouped into respective categories. Protein-protein interaction network prediction and visualization were performed using the STRING database[32].

Western Blot Analyses

Thirty μL of pooled protein samples for each group (WD1_Control, WD1_Cocaine, WD22_Control, WD22_Cocaine), as well as Prestained Protein Markers, Broad Range (Cell Signaling, Danvers, MA) were separated by SDS-PAGE using NuPAGE® Novex® 4–12% Bis-Tris Protein Gels (1.5mm, 15 well; Life Technologies, Grand Island, NY)., The separated proteins were electrophoretically transferred to nitrocellulose membranes using the iBlot system (Life Technologies) and incubated sequentially with blocking solutions (Life Technologies), primary antibodies, and secondary antibodies. The positive immunoreaction bands were detected by chemiluminescence using WesternBreeze kits (Life Technologies) and X-ray film (Thermo Scientific, San Jose, CA), and developed with a Kodak X-OMAT 2000A processor. Band intensities were quantified by Quantity One software (Bio-Rad) and normalized by comparing to β-actin, the expression of which displayed only minor fluctuations among the four experimental groups. The primary antibodies used in the study were: rabbit polyclonal anti-PKA C-alpha (1:1000, Cell Signaling Technology), rabbit polyclonal anti-Phospho-PKA C (Thr197) (1:500, Cell Signaling Technology), rabbit polyclonal anti-Phospho-(Ser/Thr) PKA Substrate (1:250, Cell Signaling Technology), mouse monoclonal anti-PKC (1:2000, Sigma Aldrich), rabbit polyclonal anti-Phospho-PKC (pan) (gamma Thr 514) (1:500, Cell Signaling Technology), rabbit polyclonal anti-Phospho-(Ser) PKC Substrate (1:1000, Cell Signaling Technology), rabbit monoclonal anti-Cofilin-1 (1:1000, Cell Signaling Technology), rabbit monoclonal anti-Phospho-Cofilin (Ser3) (1:200, Cell Signaling Technology), and mouse monoclonal anti-actin (1:5,000, Sigma Aldrich).

RESULTS & DISCUSSION

Consideration of Animal Models

In this study, we utilized a well-established cocaine withdrawal model, in which cocaine was administered in an experimenter-determined regimen. This model is easy to manipulate and monitor, and the desired endpoints are achieved within a short duration. A large number of studies have employed this well-characterized model successfully to represent cocaine withdrawal in animals[26]. We considered a second ubiquitous model for the development of cocaine dependence that is based upon self-administration, which takes into account of the “motives” of animals to intake drugs[33]. However, the self administration model is susceptible to large biological variability because individual animals may adopt different self-administration patterns, resulting in significant variations in the total amount of drug each animal administers. Therefore, we selected the experimenter-administration model to investigate the effects of short- and long-term cocaine withdrawal on the rat striatal

proteome under conditions in which individual and total doses were controlled in frequency and amount.

Large-Scale and Reproducible Ion-Current-Based MS1 Strategy for Profiling Rat Striatum

To investigate comprehensively how short- and long-term cocaine withdrawal modulates molecular networks in the striatum, a proteomics strategy enabling accurate and precise profiling of relatively small changes in protein abundance is highly desirable. Additionally, given the potential for significant inter-individual variation in this system, the capability of using larger numbers of biological replicates in a single experiment, and achieving quantification with low missing value rates is indispensable. Furthermore, evaluation of the false discovery rate for of altered proteins and its minimization addresses an important and under-appreciated problem for quantitative proteomics[21]. To this end, an ion-current-based MS1 approach developed in-house, shown in schematic form in Figure 1, was selected to fulfill the demands of this study[34–37]. Each step of the workflow was well controlled in order to achieve high quantitative accuracy and precision, low missing values rates, as well as reliable discovery of altered proteins in the striatal samples.

The sample preparation strategy was comprised of an effective protein extraction methods that utilized a strong detergent cocktail buffer and an exhaustive and reproducible SOD procedure[38]. This straightforward but highly efficient approach is superior to other prevalent sample preparation methods in terms of peptide recovery and reproducibility[38]. The mean peptide recovery achieved here was 88.0%, with a RSD of 9.1%, and day-to-day reproducibility was also excellent (data not shown). Such a high level of recovery and reproducibility provides a solid foundation for reliable LC-MS and quantitative analysis. The analysis strategy employed high-resolution and highly reproducible nanoLC separation (on a 1-meter-long column packed with small particles) coupled to an Orbitrap analyzer that was operated in an “overfilling” mode was utilized for exquisite separation and sensitive analysis of tryptic peptides derived from striatal proteins. The details and advantages of this unique strategy have been described in detail in several previous publications[35, 39–42]. A representative base peak chromatogram of high-resolution separation of the striatum digest is shown in Supplementary Figure S-1. Typically, the peptide elution window was > 330 min, with an average peak width of < 30 s (FWHM) and a peak capacity of > 600. Such an extensive separation enabled in-depth investigation of the striatal proteome, especially for low-abundance regulatory proteins. We also assessed run-to-run reproducibility by performing 20 consecutive analyses of a pooled sample over a 6-day period. Fifteen representative peptides randomly selected within each 20-min segments of the elution window were used for the evaluation. The reproducibility for the 20 7-hr runs was excellent, as demonstrated by low variations in retention times and AUC (0.1–1.4% and 8.7–14.5%, respectively) of the 15 peptide sets (data not shown). The ion-current-based MS1 approach developed in our lab[36, 39] was selected over the spectral counting method because of its better quantitative performance. Previously we have demonstrated that this ion-current-based MS1 method achieved better sensitivity, accuracy, and run-to-run reproducibility of protein quantification, with extremely low levels of missing values on either the peptide or protein level[35, 36, 42, 43]. To examine whether the ion-current-based method provides better quantification of the striatal proteome than the spectral counting method, we evaluated tboth

using the Experimental Null sample set (details in *Materials & Methods*). Representative data are shown in Figure 2. Figure 2a shows the correlation of ion peak areas and unique spectral counts for each protein of three randomly-selected pairs of replicate analyses from a pooled control sample. Each dot represents the quantitative value of a unique protein. Although the correlation (and thus the quantitative reproducibility) of high-abundance proteins are excellent for both methods, the ion-current-based approach achieved substantially better run-to-run reproducibility for the lower-abundance proteins (i.e., the data points having low quantitative values). In addition, we picked 7 housekeeping proteins, consisting of β-actin (ACTB) and 6 tubulins (TBBs), and examined the individual quantitative values among all 20 replicates (Figure 2b). Most proteins exhibited much lower quantitative variation with the ion-current-based method, confirming its superior quantitative precision.

Determination of the Optimal Cutoff Thresholds for Significantly Altered Proteins

With the optimized proteomic strategy described above, we were able to quantify 2,048 non-redundant proteins in the striatum from all 40 animals, with an FDR of <0.2% for peptide identification (Supplementary Table S-1). At least two unique peptides were required for each quantifiable protein, and a very low level of missing quantitative values was achieved; <0.3% of all quantifiable proteins have missing value in any of the biological replicates, which enables reliable quantification and statistical analysis in all subjects.

We next sought to determine significantly altered proteins in both WD1 and WD22. Because biologically meaningful changes in protein abundance were expected to be small in the animal model system, reasonable cutoff thresholds that ensure reliable discovery of changed proteins, with a low false-positive rate, are extremely critical. Therefore, we employed an Experimental Null (EN) method, described recently by our lab[37], which allows pragmatic estimation of False Altered-protein Discovery Rate (FADR) in the experiment. The EN sample set contains 20 aliquots of pooled control (non-dosed) animal samples randomly assigned into two groups that were compared with each other. Consequently, any significantly altered protein resulting from the comparison of the two EN groups is a false-positive discovery arising from technical variability. Quantitative results for the EN dataset are shown in Supplementary Table S-2. The ratio of the number of altered proteins in the EN set vs. that in the experimental set is defined as the FADR. Cutoffs for protein expression ratios and p-values were optimized to obtain a low FADR while maximizing the sensitivity of discovery. Compared with several previous statistical approaches[44, 45] that mostly target the “multiple testing problem”, the EN strategy evaluates variations of the overall analytical pipeline, thus affording a more comprehensive and accurate estimation of the FADR[37]. Moreover, the EN method not only enables the evaluation of the credibility of discovery, but also offers a quantitative index for determining ideal cutoff thresholds for significantly altered proteins. In the current study, the lowest FADR, 0.775% for WD1 and 2.70% for WD22, was obtained with a cutoff threshold of >25% change (protein ratio > 1.25 or < 0.8 and p-value <0.05 between control and treatment groups). As a result, these were selected as the thresholds for significantly altered proteins. A volcano plot for the EN sample set and FADRs achieved under different cutoff thresholds are shown in Supplementary Figure S-2. The low FADR, at such a low cutoff ratio, demonstrates the excellent capability of the

quantitative method developed to detect small magnitude changes reliably, and was achieved by the highly reproducible sample preparation and LC-MS analysis, as well as the optimized data processing procedures[36, 38, 43].

Under the optimized thresholds, a total of 129 and 37 proteins were altered significantly in WD1 and WD22 groups, respectively (Supplementary Table S-3 & S-4). The average fold changes of significantly altered proteins for WD1 and WD22 are 1.38 and 1.33 respectively (Supplementary Figure S-3). Interestingly, it was observed that short- and long-term withdrawals induced quite different protein changes. In WD1, 72.9% (94/129) of the differential proteins showed increased expression while in WD22 only 18.9% (7/37) of the differentially expressed proteins were up-regulated. Also, among the altered proteins discovered in the WD1 and WD22 groups, only 13 were in common. Although we did observe distinct proteome patterns with short- and long-term cocaine withdrawal, one important consideration is whether these statistically significant proteins are biologically meaningful, because the overall protein changes are relatively small. In fact, changes in brain proteome patterns, even under severe pathological conditions, are thought to be subtle, a notion that is supported by several previous studies. For example, more than 70 percent of cortex and cerebellum protein changes fell within 1.2–1.8 fold in a series of human prion diseases[46]. In another study, the average fold change of the 22 most significantly altered proteins (both up- and down-regulated) was 1.62 in the substantia nigra of Parkinson's disease patients compared with neurologically intact controls[47]. In the current model, in which the major stimulant (i.e. cocaine) and its secondary metabolites have been cleared from the body for a comparatively long period of time, it is very likely that that the extent of protein changes are even smaller than observed in more extreme disease states. Therefore, we extrapolate that the statistically significant changes in protein levels are biological relevant in this cocaine withdrawal model.

Functional Annotation of Significantly Altered proteins

Using the DAVID bioinformatics tool, the total- and altered protein datasets were annotated with GO analysis. Among the 2048 quantified proteins, 1343 have entries with GO terms as dictated by DAVID. We examined the biological processes and cellular components for quantified and altered proteins (Figure 3). A wide range of biological processes closely associated the cellular responses to cocaine exposure and withdrawal were revealed, including signaling cascades, vesicle-mediated transport, oxidation/reduction, phosphorylation, cytoskeleton organization, synaptic transmission behavior, cell morphogenesis, apoptosis, glucose metabolism, protein folding, oxidative stress, and neurotransmitter metabolism. The details of proteins altered in each category are listed in Supplementary Table S-5. Most of these biological processes are associated with signal transduction, neurotransmission, and neuroplasticity, implicating the CNS-specific roles of these changes. These proteins are also from various subcellular localizations (Figure 3); notably, 41.70% (560/1343) of all proteins were derived from the membranous fractions (i.e. plasma and organelle membranes). This reflects the fact that a large proportion of proteins in cerebral tissues are membrane proteins, and results from the fact that our sample preparation procedures achieved excellent recovery of membrane proteins.

We utilized the STRING database to construct protein-protein interaction networks for significantly altered proteins in WD1 and WD22. For WD1, several key “sub-networks”, highlighted by different colored circles, were identified (Supplementary Figure S-4). These include proteins involved in: 1) glucose metabolism and energy production (red); 2) calcium signaling and vesicle transport (orange); 3) neurotransmitter metabolism (yellow); 4) stress response (green); 5) 14-3-3 signaling (blue); 6) G-protein signaling, cAMP signaling and actin cytoskeleton (purple). The interaction network of WD22 is shown in Supplementary Figure S-5. Combining the results from both GO analysis and the STRING database, we identified a collection of proteins that are potentially relevant to the molecular alterations after short- and long-term cocaine withdrawal. These proteins were classified into a variety of functional categories as shown in Table 1. The majority of these proteins exhibited changed levels in WD1 and were normalized to baseline levels in WD22, which suggested that most acute molecular-level effects induced by cocaine exposure faded with prolonged cocaine withdrawal. By contrast, a few proteins were significantly dysregulated in WD22 compared to age-matched controls, suggesting that molecular changes could be imprinted in a cocaine-addicted brain with long-term cocaine withdrawal. These results are consistent with a large number of previous reports, and support the likelihood that this proteomics profiling strategy has successfully recapitulated the altered proteome patterns that follow short and long periods of withdrawal from cocaine when many symptoms of cocaine dependence emerge.

The likely biological relevance of changes in several protein categories is as follows. First, significant up-regulation of heat shock proteins (HSPs) were observed in WD1. According to literature reports, chronic cocaine administration compromises normal dopamine transporter (DAT) functions, thus posing oxidative stress on CNS and leading to elevated HSP expression[48]. This has been observed in several mammalian CNS regions, including hippocampus[48], prefrontal cortex[49] and cerebellum[50], and our results suggest that elevation of HSP expression also occurred in the striatum. Second, proteins involved in synaptic neurotransmission (e.g. neurotransmitter metabolism) were also subjected to dysregulation. The most noteworthy change was the significantly increased levels of the sodium-dependent DAT, which may suggest a compensatory response to the loss of striatal DAT function as a result of chronic cocaine exposure. Several other proteins involved in glutamate and GABA metabolism were also up-regulated in WD1. The increase in these proteins likely reflect intensified glutamatergic and GABAergic neurotransmission in the striatum, which are the predominant changes during and after the formation of cocaine dependence[26, 51]; striatum appears to be the primary hub orchestrating the interactions between these neurotransmission types[52]. Third, more than ten proteins involved in glucose metabolism also displayed differential expression in WD1. Several studies have reported that cocaine inhibits regional/global glucose metabolism in various mammalian subjects including human cocaine users[53], non-human primates[54], and rodents[55]. We hypothesize that the increased glucose metabolism proteins observed might serve to rescue the deterioration of energy production caused by chronic cocaine exposure.

Novel Biological Implications Underlying Short- and Long-Term Cocaine Withdrawal

These studies revealed changes in protein abundance that are of potential significance for the investigation of molecular mechanisms underlying short- and long-term cocaine withdrawal. These changed proteins and their biological implications are described below.

Prolonged PKC Activation during Cocaine Withdrawal—Proteins involved in G protein signaling and Ca^{2+} signaling were significantly altered, mostly in WD1. These signaling pathways have been reported to be parts of the molecular machineries affecting neuroplasticity and inducing behavioral sensitization post chronic psychostimulant exposure. Alteration in G protein and Ca^{2+} signaling pathways could lead to the activation of two ubiquitous protein kinases – protein kinase A (PKA) and protein kinase C (PKC)[56], which are regarded as important components in structural plasticity during psychostimulant exposure[57]. PKA and PKC were also found to contribute to the consolidation of stimulus-reward association that affects critically the behaviors of rats under cocaine place conditioning[58]. Increased levels of adenylate cyclase (AC) type 5 and the protein kinase A (PKA) regulatory subunit were observed in WD1 but not in WD22. However, PKA catalytic subunit (PKA C), the key determinant of PKA activity, was not identified in the proteomics analysis. To explore whether PKA activity was altered, we performed Western blot analysis of total PKA C-α and phospho-PKA C in both WD1 and WD22. Surprisingly, there was no significantly change of either total PKA C-α or phospho-PKA C in both cocaine treated groups (WD1 and WD22), compared with their age-matched controls (Supplementary Figure S-6). Additionally, phospho-PKA substrate bands also showed no significant change in the WD1 or WD22 groups (data not shown). These results implied that PKA activity may not be changed significantly in rat striatum after repeated cocaine exposure and withdrawal, despite the fact that elevation of AC was observed. Although our results may appear contradictory with previous resulting finding that PKA activity in brain regions such as the nucleus accumbens (NAc) is activated after cocaine exposure and may orchestrate structural plasticity by subsequently activation of cAMP-responsive element binding protein (CREB)[9], a recent study showed that consecutive injections of amphetamine or cocaine resulted in reduced accumbal PKA activity, whereas repeated cocaine treatment plus withdrawal did not alter dorsal striatal PKA activity[59]. Therefore, cocaine-induced alteration of PKA activity may depend upon the pattern of drug administration, the presence of withdrawal, and the specific brain regions.

PKC also plays a versatile role during cocaine exposure and withdrawal. For example, intact PKC is required for cocaine to inhibit dopamine release during acute cocaine exposure[60], and DAT phosphorylation states and activity are also regulated by PKC[61]. Therefore, the expression and activity of total PKC, phospho-PKC, and phospho-PKC substrates were examined by Western blots. Although total PKC displayed no significant alterations at either time point, elevated phospho-PKC levels were observed in WD1 (1.67 ± 0.13) and persisted in WD22 (2.23 ± 0.30), compared to their respective controls (Figure 4a & 4b). In terms of phospho-PKC substrates, no significant changes was revealed in the WD1 group, but significant increases were observed in the WD22 group (Figure 4c), as is suggested by the higher intensity for almost all putative bands detected in the assay (Supplementary Figure S-7). The intensity of three representative bands in different molecular weight ranges are

also compared for the treated *vs.* control WD22 groups, and significantly higher levels of phosphorylation were observed in the cocaine withdrawal group (Band 1: 1.93 ± 0.16; Band 2: 1.61 ± 0.19; Band 3: 2.10 ± 0.22; Figure 4d). These results correspond with the higher phospho-PKC levels in WD22. In agreement with these results, Li et al. demonstrated that inhibition of PKMzeta, an atyptical PKC isozyme, abolished the long-term drug reward memory in NAc[62]. Another study showed that the reversal of cocaine-induced behavioral sensitization correlated with the reversal of striatum-specific GABAergic system functions and PKC activity[63]. In summary, increased PKC, but not PKA, activity was detected in rat striatum with both short- or long-term cocaine withdrawal, indicating that striatal PKC may be activated persistently after chronic cocaine exposure, even when cocaine has been largely cleared from the system.

Altered Actin Cytoskeleton Reorganization during Cocaine Withdrawal— Cytoskeleton reorganization allows morphological modifications of cellular and subcellular structures, and is the fundamental basis for structural plasticity[64, 65]. Dysregulated cytoskeleton protein levels have been reported after exposure to cocaine and other psychostimulants by previous studies[66]. From our results, fourteen proteins constituting or regulating all three types of cytoskeleton filaments (actin filaments, intermediate filaments (IF) and microtubules) underwent changes in expression, indicating active cytoskeleton reorganization in striatal neuronal cells after cocaine exposure and withdrawal. Actin filament and microtubule proteins were up-regulated in WD1, whereas IF proteins were down-regulated in WD1. These findings agree with an earlier study showing that IF levels were negatively regulated in the ventral tegmental area with chronic morphine or cocaine use[67]. Moreover, most of these proteins were normalized to baseline levels in WD22, with the sole exception of cofilin-1 (non-muscle form of cofilins), which was altered in both the WD1 and WD22 groups. As a member of the actin-binding proteins, which promote assembly and disassembly of actin filaments, cofilin-1 functions to convert actin filaments into monomers and increase actin turnover, thus facilitating the reshaping of the actin cytoskeleton[68]. In the CNS, cofilin-1 has been proposed to play an important role during drug-induced neuroplasticity by regulating the density and morphology of dendritic spines via actin cytoskeleton reorganization, and changes in expression and activity during cocaine stimulation[69, 70].

Under this context, we examined both total cofilin-1 and phospho-cofilin-1 (i.e. the inactive cofilin-1 form) levels by Western blot. As shown in Figure 5, p-cofilin-1 levels were decreased significantly in WD1 (0.64 ± 0.13, $p < 0.05$) and increased in WD22 (1.95 ± 0.28, $p < 0.05$). This finding suggests reinforced cofilin-1 activity in WD1 and attenuated cofilin-1 activity in WD22, from which it could be further deduced that actin turnover might be enhanced immediately after termination of chronic cocaine exposure (e.g. after 1 day withdrawal) and suppressed after extended cocaine withdrawal (e.g. 22 days). Previously, Dietz et al. discovered that repeated cocaine treatment was associated with significant decreases of p-cofilin *via* a Rac1-dependent signaling pathway in the NAc[71]. This report is consistent with our observation in WD1, wherein cofilin activity was up-regulated significantly. Toda et al. demonstrated sustained increases in actin cycling in dendritic spines of medium spiny neurons in the NAc with chronic cocaine exposure, accompanied by

alterations in p-cofilin and LIMK levels[70]. Interestingly, although that study found decreased NAc p-cofilin levels with 22-day withdrawal, we observed increased striatal p-cofilin levels after a similar length of cocaine withdrawal, thus suggesting location-specific changes in cytoskeleton turnover. In summary, our results suggest a more dynamic striatal actin cytoskeleton shortly after chronic cocaine exposure, as well a more static actin cytoskeleton after a considerably long period of cocaine withdrawal. These changes likely reflect the altered neuroplasticity during cocaine exposure and withdrawal.

Potential Vasoconstriction during Long-Term Cocaine Withdrawal—The results show that five red blood cell (RBC) and plasma proteins, including zero beta globin, hemoglobin, and albumin were differentially expressed (Figure 6). Interestingly, although they were elevated in WD1, all were decreased significantly in WD22. Because the animals were not perfused upon sacrifice to remove blood from the organs, it is reasonable to assume the abundance of blood proteins is proportional to the amount of blood, and therefore the vessel volumes, in the tissues. Therefore, the results suggest drastic fluctuations in vessel volumes after cocaine exposure and short- *vs.* long-term withdrawal. Vasodilation and vasoconstriction are regarded among the most prevalent side effects of chronic cocaine use[72]. In fact, cardiovascular and cerebrovascular complications such as myocardial ischemia and infarction[73], atherosclerosis[74], ischemic stroke[75], and intracerebral hemorrhage[76] are commonly diagnosed among chronic cocaine users, and cocaine-induced vasoconstriction may be an important contributing factor. However, the temporal features of the onset and development of vasoconstriction have not been elucidated previously. Here, the significant elevation of blood-related proteins in WD1 suggest the cocaine exposure may have caused temporary vasodilation. Conversely, the decrease in blood-related proteins in WD22 suggests vasoconstriction in the striatum after long-term withdrawal. Therefore, vasoconstrictive effects associated with chronic cocaine use represent the aftermath of prolonged withdrawal rather than prolonged exposure, given that the decrease of blood proteins were observed in WD22 but not in WD1.

CONCLUSION

In summary, an ion-current-based MS1 approach developed in-house enabled large-scale, quantitative proteomic profiling of the striatum in rats chronically exposed to cocaine and subjected to two distinct durations of cocaine withdrawal. The proteomic strategy was thoroughly optimized to achieve comprehensive, reproducible, and high-throughput analysis of striatal samples from 40 subjects. By identifying and applying optimal cutoff thresholds determined by our EN strategy, we confidently identified myriad significant changes in the abundance of cellular proteins associated with 1d and 22d of cocaine withdrawal. The nature of these protein changes suggest significant impact if cocaine exposure and withdrawal upon a wide range of biological processes, including signaling cascades, vesicle-mediated transport, oxidation reduction, phosphorylation, cytoskeleton organization, and synaptic transmission. The proteomic results, coupled with ancillary immunoassays, revealed interesting regulatory processes coordinated by protein kinase activities, as well as actin cytoskeleton reorganization. These observations may provide new insights into the cocaine-seeking behaviors and neuroplasticity changes induced by short- and longer term cocaine

withdrawal. The temporal changes in protein levels and activities, in response to different lengths of cocaine withdrawal, appeared to corroborate with the behavioral features in this period. Additionally, the observed decline in blood proteins suggest the occurrence of vasoconstriction after long-term, but not short-term cocaine withdrawal, which may have importance for the clinical treatment of cocaine-induced cardiovascular complications. Studies to explore these correlations further are ongoing. Most importantly, this work demonstrated a proteomics pipeline that can be applied to the large-scale comparative investigation of brain tissues and other biological systems in which the investigation of many biological replicates in one set is desirable.

Supplementary Material

Refer to Web version on PubMed Central for supplementary material.

Acknowledgments

This work was supported in part by NIH grants U54HD071594 (JQ) and HL103411 (JQ), DA027528 (JQ, ACT, RMS) and DA020261 (ACT) from the National Inst. on Drug Abuse, a Center of Protein Therapeutics Industrial Award (JQ), and American Heart Association (AHA) award 12SDG9450036 (JQ).

ABBREVIATIONS

ACTB	β-actin
ADF	actin depolymerization factor
AF	actin filament
BBB	blood-brain barrier
BCA	bicinchoninic acid assay
CNS	central nervous system
DAT	dopamine transporters
DAVID	the Database for Annotation, Visualization and Integrated Discovery
D1R/D2R	dopamine D1/D2 receptor
EN	Experimental Null
FA	formic acid
FDR	false discovery rate
GAP43	growth associated protein 43
GO	gene ontology
HSP	heat shock protein
IAM	iodoacetamide

IF	intermediate filament
NAc	nucleus accumbens
PKA	protein kinase A
PKC	protein kinase C
RBC	red blood cell
SOD	surfactant-aided precipitation/on-pellet digestion
TBB	tubulin
TCEP	tris(2-carboxyl)phosphine
TIC	total ion current
WD1	1 day cocaine withdrawal
WD22	22 day cocaine withdrawal

References

1. Association, A. P. Diagnostic and statistical manual of mental disorders. 4. American Psychiatric Association; Washington, DC: 1994.
2. Karila L, Petit A, Lowenstein W, Reynaud M. Diagnosis and consequences of cocaine addiction. Curr Med Chem. 2012
3. Roldan CA, Aliabadi D, Crawford MH. Prevalence of heart disease in asymptomatic chronic cocaine users. Cardiology. 2001; 95:25–30. [PubMed: 11385188]
4. Yakel DL Jr, Eisenberg MJ. Pulmonary artery hypertension in chronic intravenous cocaine users. Am Heart J. 1995; 130:398–9. [PubMed: 7631626]
5. Karila L, Reynaud M, Aubin HJ, Rolland B, Guardia D, Cottencin O, Benyamina A. Pharmacological treatments for cocaine dependence: is there something new? Curr Pharm Des. 2011; 17:1359–68. [PubMed: 21524259]
6. Dittmar PK, Olmedo R. An Evidence-Based Approach To Cocaine-Associated Emergencies. Emergency Medicine Practice. 2008; 10:1–19.
7. Wagner FA, Anthony JC. From first drug use to drug dependence; developmental periods of risk for dependence upon marijuana, cocaine, and alcohol. Neuropsychopharmacology. 2002; 26:479–88. [PubMed: 11927172]
8. Luscher C, Malenka RC. Drug-evoked synaptic plasticity in addiction: from molecular changes to circuit remodeling. Neuron. 2011; 69:650–63. [PubMed: 21338877]
9. Dietz DM, Dietz KC, Nestler EJ, Russo SJ. Molecular mechanisms of psychostimulant-induced structural plasticity. Pharmacopsychiatry. 2009; 42(Suppl 1):S69–78. [PubMed: 19434558]
10. Waselus M, Flagel SB, Jedynak JP, Akil H, Robinson TE, Watson SJ Jr. Long-term effects of cocaine experience on neuroplasticity in the nucleus accumbens core of addiction-prone rats. Neuroscience. 2013; 248:571–584. [PubMed: 23811073]
11. Koob GF, Ahmed SH, Boutrel B, Chen SA, Kenny PJ, Markou A, O'Dell LE, Parsons LH, Sanna PP. Neurobiological mechanisms in the transition from drug use to drug dependence. Neurosci Biobehav Rev. 2004; 27:739–49. [PubMed: 15019424]
12. Hemby SE, Tannu N. Modeling substance abuse for applications in proteomics. Methods Mol Biol. 2009; 566:69–83. [PubMed: 20058165]
13. Iwazaki T, McGregor IS, Matsumoto I. Protein expression profile in the striatum of acute methamphetamine-treated rats. Brain Res. 2006; 1097:19–25. [PubMed: 16729985]

14. Reynolds JL, Mahajan SD, Bindukumar B, Sykes D, Schwartz SA, Nair MP. Proteomic analysis of the effects of cocaine on the enhancement of HIV-1 replication in normal human astrocytes (NHA). Brain Res. 2006; 1123:226–36. [PubMed: 17034766]
15. Reissner KJ, Uys JD, Schwacke JH, Comte-Walters S, Rutherford-Bethard JL, Dunn TE, Blumer JB, Schey KL, Kalivas PW. AKAP signaling in reinstated cocaine seeking revealed by iTRAQ proteomic analysis. J Neurosci. 2011; 31:5648–58. [PubMed: 21490206]
16. Kim SI, Voshol H, van Oostrum J, Hastings TG, Cascio M, Glucksman MJ. Neuroproteomics: expression profiling of the brain's proteomes in health and disease. Neurochem Res. 2004; 29:1317–31. [PubMed: 15176488]
17. Fisk JC, Li J, Wang H, Aletta JM, Qu J, Read LK. Proteomic Analysis Reveals Diverse Classes of Arginine Methylproteins in Mitochondria of Trypanosomes. Mol Cell Proteomics. 2012
18. Keshishian H, Addona T, Burgess M, Kuhn E, Carr SA. Quantitative, multiplexed assays for low abundance proteins in plasma by targeted mass spectrometry and stable isotope dilution. Mol Cell Proteomics. 2007; 6:2212–29. [PubMed: 17939991]
19. Gilmore JM, Washburn MP. Advances in shotgun proteomics and the analysis of membrane proteomes. J Proteomics. 2010; 73:2078–91. [PubMed: 20797458]
20. Mets B, Diaz J, Soo E, Jamdar S. Cocaine, norcocaine, ecgonine methylester and benzoylecgonine pharmacokinetics in the rat. Life Sci. 1999; 65:1317–28. [PubMed: 10503947]
21. Carr SA, Anderson L. Protein quantitation through targeted mass spectrometry: the way out of biomarker purgatory? Clin Chem. 2008; 54:1749–52. [PubMed: 18957555]
22. Rifai N, Gillette MA, Carr SA. Protein biomarker discovery and validation: the long and uncertain path to clinical utility. Nat Biotechnol. 2006; 24:971–83. [PubMed: 16900146]
23. Nesvizhskii AI. A survey of computational methods and error rate estimation procedures for peptide and protein identification in shotgun proteomics. J Proteomics. 2010; 73:2092–123. [PubMed: 20816881]
24. Fowler JS, Volkow ND, Wolf AP, Dewey SL, Schlyer DJ, Macgregor RR, Hitzemann R, Logan J, Bendriem B, Gatley SJ, et al. Mapping cocaine binding sites in human and baboon brain in vivo. Synapse. 1989; 4:371–7. [PubMed: 2557686]
25. Everitt BJ, Wolf ME. Psychomotor stimulant addiction: a neural systems perspective. J Neurosci. 2002; 22:3312–20. [PubMed: 11978805]
26. Kuhar MJ, Pilotte NS. Neurochemical changes in cocaine withdrawal. Trends Pharmacol Sci. 1996; 17:260–4. [PubMed: 8756185]
27. Chiu K, Lau WM, Lau HT, So K, Chang RC. Micro-dissection of rat brain for RNA or protein extraction from specific brain region. Journal of Visualized Experiments. 2007
28. Searle BC. Scaffold: a bioinformatic tool for validating MS/MS-based proteomic studies. Proteomics. 2010; 10:1265–9. [PubMed: 20077414]
29. Elias JE, Haas W, Faherty BK, Gygi SP. Comparative evaluation of mass spectrometry platforms used in large-scale proteomics investigations. Nat Methods. 2005; 2:667–75. [PubMed: 16118637]
30. Lopez MF, Kuppusamy R, Sarracino DA, Prakash A, Athanas M, Krastins B, Rezai T, Sutton JN, Peterman S, Nicolaides K. Mass spectrometric discovery and selective reaction monitoring (SRM) of putative protein biomarker candidates in first trimester Trisomy 21 maternal serum. J Proteome Res. 2011; 10:133–42. [PubMed: 20499897]
31. Huang da W, Sherman BT, Lempicki RA. Systematic and integrative analysis of large gene lists using DAVID bioinformatics resources. Nat Protoc. 2009; 4:44–57. [PubMed: 19131956]
32. Jensen LJ, Kuhn M, Stark M, Chaffron S, Creevey C, Muller J, Doerks T, Julien P, Roth A, Simonovic M, Bork P, von Mering C. STRING 8--a global view on proteins and their functional interactions in 630 organisms. Nucleic Acids Res. 2009; 37:D412–6. [PubMed: 18940858]
33. Koob GF, Caine SB. Drug self-administration and microdialysis in rodents. Short CourSe I. 2007
34. Tu C, Beharry KD, Shen X, Li J, Wang L, Aranda JV, Qu J. Proteomic profiling of the retinas in a neonatal rat model of oxygen-induced retinopathy with a reproducible ion-current-based MS1 approach. J Proteome Res. 2015; 14:2109–20. [PubMed: 25780855]
35. Tu C, Li J, Jiang X, Sheflin LG, Pfeffer BA, Behringer M, Fliesler SJ, Qu J. Ion-current-based proteomic profiling of the retina in a rat model of Smith-Lemli-Opitz syndrome. Mol Cell Proteomics. 2013; 12:3583–98. [PubMed: 23979708]

36. Tu C, Sheng Q, Li J, Shen X, Zhang M, Shyr Y, Qu J. ICan: an optimized ion-current-based quantification procedure with enhanced quantitative accuracy and sensitivity in biomarker discovery. J Proteome Res. 2014; 13:5888–97. [PubMed: 25285707]
37. Shen X, Hu Q, Li J, Wang J, Qu J. An Experimental Null method to guide the development of technical procedures and to control false positive discovery in quantitative proteomics. J Proteome Res. 2015
38. An B, Zhang M, Johnson RW, Qu J. Surfactant-Aided Precipitation/on-Pellet-Digestion (SOD) Procedure Provides Robust and Rapid Sample Preparation for Reproducible, Accurate and Sensitive LC/MS Quantification of Therapeutic Protein in Plasma and Tissues. Anal Chem. 2015; 87:4023–9. [PubMed: 25746131]
39. Nouri-Nigjeh E, Sukumaran S, Tu C, Li J, Shen X, Duan X, DuBois DC, Almon RR, Jusko WJ, Qu J. Highly multiplexed and reproducible ion-current-based strategy for large-scale quantitative proteomics and the application to protein expression dynamics induced by methylprednisolone in 60 rats. Anal Chem. 2014; 86:8149–57. [PubMed: 25072516]
40. Qu J, Young R, Page BJ, Shen X, Tata N, Li J, Duan X, Fallavollita JA, Canty JM Jr. Reproducible Ion-Current-Based Approach for 24-Plex Comparison of the Tissue Proteomes of Hibernating versus Normal Myocardium in Swine Models. J Proteome Res. 2014
41. Tu C, Mammen MJ, Li J, Shen X, Jiang X, Hu Q, Wang J, Sethi S, Qu J. Large-scale, ion-current-based proteomics investigation of bronchoalveolar lavage fluid in chronic obstructive pulmonary disease patients. J Proteome Res. 2014; 13:627–39. [PubMed: 24188068]
42. Shen S, Li J, Hilchey S, Shen X, Tu C, Qiu X, Ng A, Ghaemmaghami S, Wu H, Zand MS, Qu J. Ion-Current-Based Temporal Proteomic Profiling of Influenza-A-Virus-Infected Mouse Lungs Revealed Underlying Mechanisms of Altered Integrity of the Lung Microvascular Barrier. Journal of Proteome Research. 2016; 15:540–553. [PubMed: 26650791]
43. Tu C, Li J, Sheng Q, Zhang M, Qu J. Systematic assessment of survey scan and MS2-based abundance strategies for label-free quantitative proteomics using high-resolution MS data. J Proteome Res. 2014; 13:2069–79. [PubMed: 24635752]
44. Diz AP, Carvajal-Rodriguez A, Skibinski DO. Multiple hypothesis testing in proteomics: a strategy for experimental work. Mol Cell Proteomics. 2011; 10:M110 004374.
45. Karp NA, McCormick PS, Russell MR, Lilley KS. Experimental and statistical considerations to avoid false conclusions in proteomics studies using differential in-gel electrophoresis. Mol Cell Proteomics. 2007; 6:1354–64. [PubMed: 17513293]
46. Shi Q, Chen LN, Zhang BY, Xiao K, Zhou W, Chen C, Zhang XM, Tian C, Gao C, Wang J, Han J, Dong XP. Proteomics analyses for the global proteins in the brain tissues of different human prion diseases. Mol Cell Proteomics. 2015; 14:854–69. [PubMed: 25616867]
47. Licker V, Turck N, Kovari E, Burkhardt K, Cote M, Surini-Demiri M, Lobrinus JA, Sanchez JC, Burkhard PR. Proteomic analysis of human substantia nigra identifies novel candidates involved in Parkinson's disease pathogenesis. Proteomics. 2014; 14:784–94. [PubMed: 24449343]
48. Hayase T, Yamamoto Y, Yamamoto K, Muso E, Shiota K. Stressor-like effects of cocaine on heat shock protein and stress-activated protein kinase expression in the rat hippocampus: interaction with ethanol and anti-toxicity drugs. Leg Med (Tokyo). 2003; 5(Suppl 1):S87–90. [PubMed: 12935560]
49. Lull ME, Erwin MS, Morgan D, Roberts DC, Vrana KE, Freeman WM. Persistent proteomic alterations in the medial prefrontal cortex with abstinence from cocaine self-administration. Proteomics Clin Appl. 2009; 3:462–472. [PubMed: 20161123]
50. Dietrich JB, Arpin-Bott MP, Kao D, Dirrig-Grosch S, Aunis D, Zwiller J. Cocaine induces the expression of homer 1b/c, homer 3a/b, and hsp 27 proteins in rat cerebellum. Synapse. 2007; 61:587–94. [PubMed: 17455232]
51. Porrino LJ, Daunais JB, Smith HR, Nader MA. The expanding effects of cocaine: studies in a nonhuman primate model of cocaine self-administration. Neurosci Biobehav Rev. 2004; 27:813–20. [PubMed: 15019430]
52. Karler R, Calder LD, Thai LH, Bedingfield JB. The dopaminergic, glutamatergic, GABAergic bases for the action of amphetamine and cocaine. Brain Res. 1995; 671:100–4. [PubMed: 7728520]

53. London ED, Cascella NG, Wong DF, Phillips RL, Dannals RF, Links JM, Herning R, Grayson R, Jaffe JH, Wagner HN. Cocaine-induced redoppuction of glucose utilization in human brain: A study using positron emission tomography and [Fluorine 18]-fluorodeoxyglucose. Archives of General Psychiatry. 1990; 47:567–574. [PubMed: 2350209]

54. Lyons D, Friedman DP, Nader MA, Porrino LJ. Cocaine alters cerebral metabolism within the ventral striatum and limbic cortex of monkeys. J Neurosci. 1996; 16:1230–8. [PubMed: 8558251]

55. Thanos PK, Michaelides M, Benveniste H, Wang GJ, Volkow ND. The effects of cocaine on regional brain glucose metabolism is attenuated in dopamine transporter knockout mice. Synapse. 2008; 62:319–24. [PubMed: 18286542]

56. Gilman AG. G proteins: transducers of receptor-generated signals. Annu Rev Biochem. 1987; 56:615–49. [PubMed: 3113327]

57. Surmeier DJ, Ding J, Day M, Wang Z, Shen W. D1 and D2 dopamine-receptor modulation of striatal glutamatergic signaling in striatal medium spiny neurons. Trends Neurosci. 2007; 30:228–35. [PubMed: 17408758]

58. Cervo L, Mukherjee S, Bertaglia A, Samanin R. Protein kinases A and C are involved in the mechanisms underlying consolidation of cocaine place conditioning. Brain Res. 1997; 775:30–6. [PubMed: 9439825]

59. Crawford CA, Choi FY, Kohutek JL, Yoshida ST, McDougall SA. Changes in PKA activity and Gs alpha and Golf alpha levels after amphetamine- and cocaine-induced behavioral sensitization. Synapse. 2004; 51:241–8. [PubMed: 14696012]

60. Nuwayhid SJ, Werling LL. Sigma2 (sigma2) receptors as a target for cocaine action in the rat striatum. Eur J Pharmacol. 2006; 535:98–103. [PubMed: 16480713]

61. Gorentla BK, Vaughan RA. Differential effects of dopamine and psychoactive drugs on dopamine transporter phosphorylation and regulation. Neuropharmacology. 2005; 49:759–68. [PubMed: 16181646]

62. Li YQ, Xue YX, He YY, Li FQ, Xue LF, Xu CM, Sacktor TC, Shaham Y, Lu L. Inhibition of PKMzeta in nucleus accumbens core abolishes long-term drug reward memory. J Neurosci. 2011; 31:5436–46. [PubMed: 21471379]

63. Chen Q, Lee TH, Wetsel WC, Sun QA, Liu Y, Davidson C, Xiong X, Ellinwood EH, Zhang X. Reversal of cocaine sensitization-induced behavioral sensitization normalizes GAD67 and GABAA receptor alpha2 subunit expression, and PKC zeta activity. Biochem Biophys Res Commun. 2007; 356:733–8. [PubMed: 17382295]

64. Carlisle HJ, Kennedy MB. Spine architecture and synaptic plasticity. Trends Neurosci. 2005; 28:182–7. [PubMed: 15808352]

65. Russo SJ, Dietz DM, Dumitriu D, Morrison JH, Malenka RC, Nestler EJ. The addicted synapse: mechanisms of synaptic and structural plasticity in nucleus accumbens. Trends Neurosci. 2010; 33:267–76. [PubMed: 20207024]

66. Lee CT, Lehrmann E, Hayashi T, Amable R, Tsai SY, Chen J, Sanchez JF, Shen J, Becker KG, Freed WJ. Gene expression profiling reveals distinct cocaine-responsive genes in human fetal CNS cell types. J Addict Med. 2009; 3:218–26. [PubMed: 20948987]

67. Beitner-Johnson D, Guitart X, Nestler EJ. Neurofilament proteins and the mesolimbic dopamine system: common regulation by chronic morphine and chronic cocaine in the rat ventral tegmental area. J Neurosci. 1992; 12:2165–76. [PubMed: 1376774]

68. Arber S, Barbayannis FA, Hanser H, Schneider C, Stanyon CA, Bernard O, Caroni P. Regulation of actin dynamics through phosphorylation of cofilin by LIM-kinase. Nature. 1998; 393:805–9. [PubMed: 9655397]

69. Kim WY, Shin SR, Kim S, Jeon S, Kim JH. Cocaine regulates ezrin-radixin-moesin proteins and RhoA signaling in the nucleus accumbens. Neuroscience. 2009; 163:501–5. [PubMed: 19580848]

70. Toda S, Shen HW, Peters J, Cagle S, Kalivas PW. Cocaine increases actin cycling: effects in the reinstatement model of drug seeking. J Neurosci. 2006; 26:1579–87. [PubMed: 16452681]

71. Dietz DM, Sun H, Lobo MK, Cahill ME, Chadwick B, Gao V, Koo JW, Mazei-Robison MS, Dias C, Maze I, Damez-Werno D, Dietz KC, Scobie KN, Ferguson D, Christoffel D, Ohnishi Y, Hodes GE, Zheng Y, Neve RL, Hahn KM, Russo SJ, Nestler EJ. Rac1 is essential in cocaine-induced

structural plasticity of nucleus accumbens neurons. Nat Neurosci. 2012; 15:891–6. [PubMed: 22522400]

72. Schwartz BG, Rezkalla S, Kloner RA. Cardiovascular Effects of Cocaine. Circulation. 2010; 122:2558–2569. [PubMed: 21156654]
73. Lange RA, Hillis LD. Cardiovascular complications of cocaine use. N Engl J Med. 2001; 345:351–8. [PubMed: 11484693]
74. Kloner RA, Hale S, Alker K, Rezkalla S. The effects of acute and chronic cocaine use on the heart. Circulation. 1992; 85:407–19. [PubMed: 1346509]
75. Levine SR, Washington JM, Jefferson MF, Kieran SN, Moen M, Feit H, Welch KM. "Crack" cocaine-associated stroke. Neurology. 1987; 37:1849–53. [PubMed: 3683875]
76. Brown E, Prager J, Lee HY, Ramsey RG. CNS complications of cocaine abuse: prevalence, pathophysiology, and neuroradiology. AJR Am J Roentgenol. 1992; 159:137–47. [PubMed: 1609688]

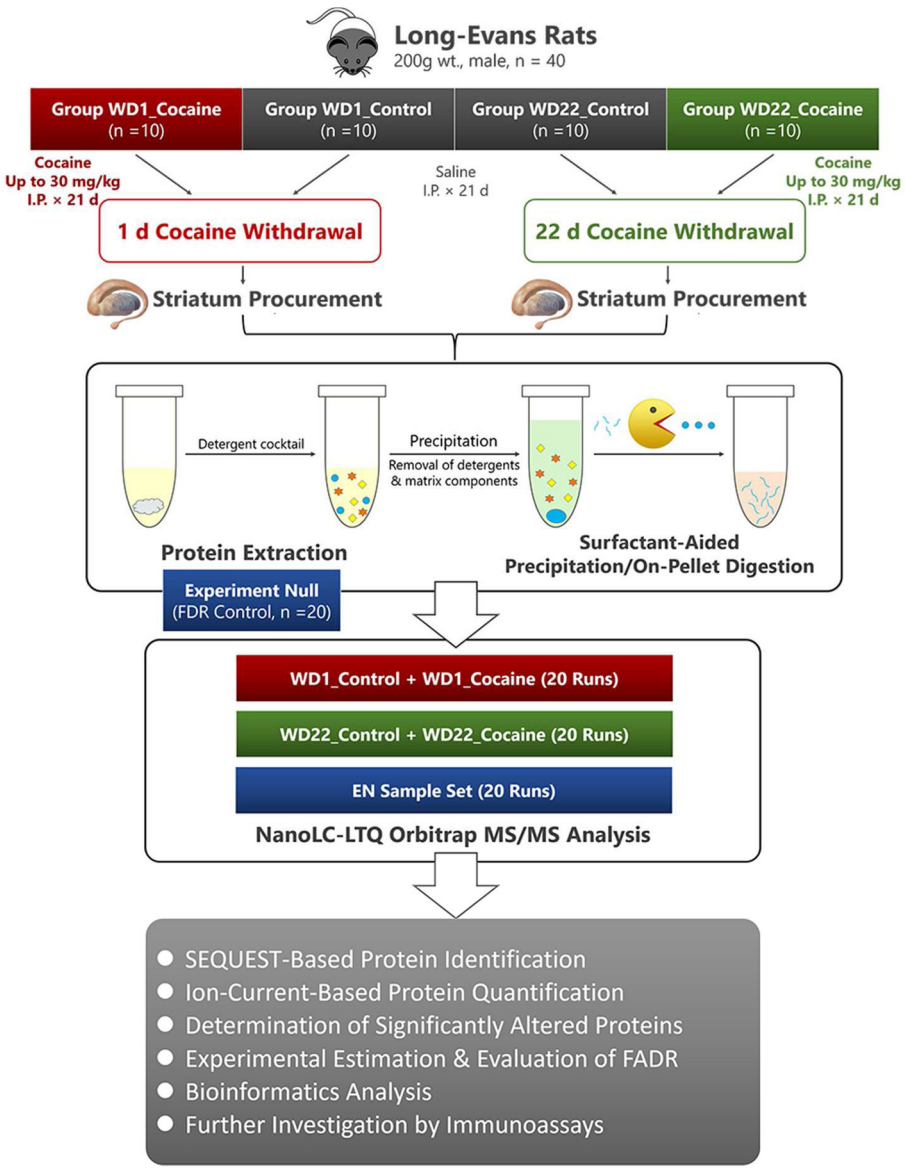

Figure 1.

Schematic illustration of the overall proteomic strategy for the quantitative expression profiling of striatum tissues from rats with 21 d cocaine exposure and 1 d/22 d withdrawal versus age-matched saline controls (n = 10 per group, 40 in total). A well-controlled and optimized ion-current-based approach with excellent quantitative accuracy and reproducibility, as well as high capacity for biological replicates, was employed. FADR were estimated and controlled by the involvement of an experimental null (EN) sample set.

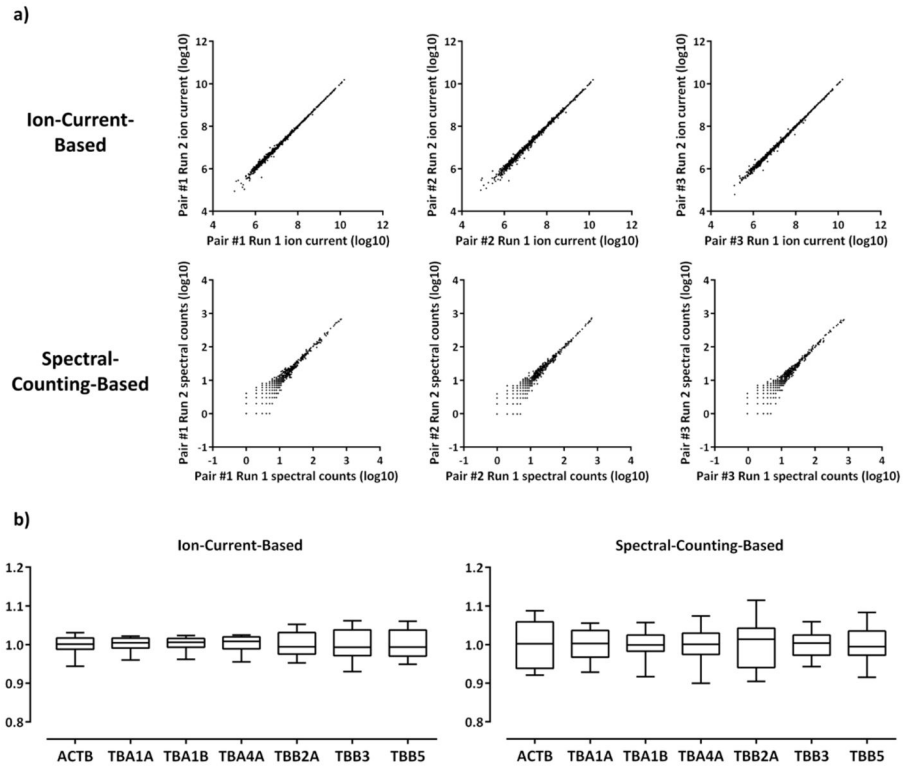

Figure 2. Evaluation of analytical reproducibility by comparing our ion-current-based approach with the spectral counting one, by replicate analysis of the same pooled sample

a) Comparison of quantitative reproducibility between MS1 ion current and MS2 spectral counts, using three randomly-selected pairs from the 20 replicates in the EN sample set; b) Quantitative values of 7 common housekeeping proteins (ACTB, TBA1A, TBA1B, TBA4A,TBB2A,TBB3, TBB5) among the 20 technical replicates.

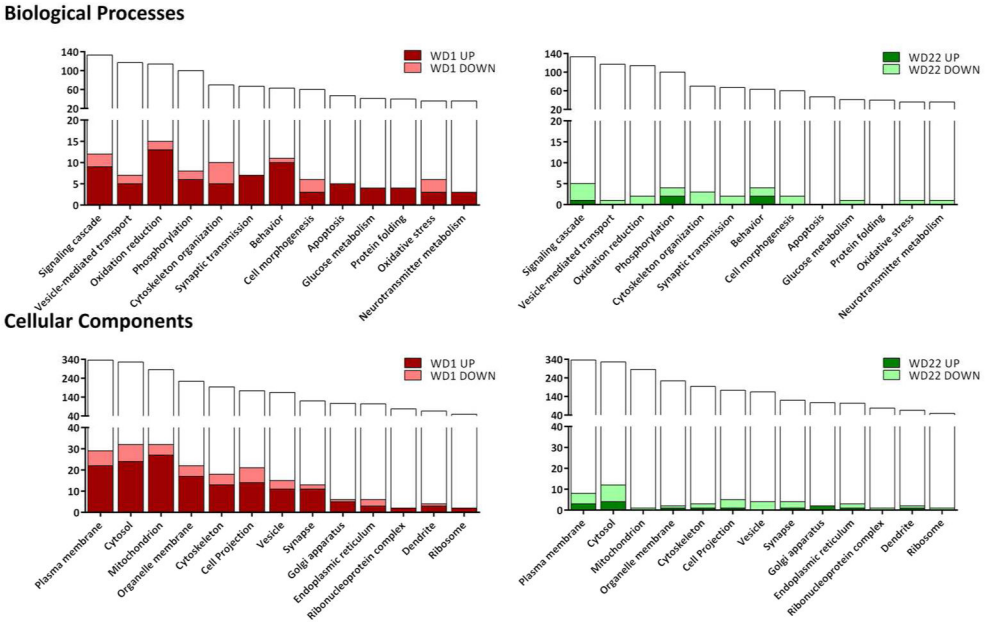

Figure 3.

Functional annotation (GO biological processes & cellular components) of the proteins quantified. Functional categories were picked manually from the results returned by DAVID. White bars refer to the total number of proteins in each category, whereas colored bars denote the fractions of significantly altered proteins.

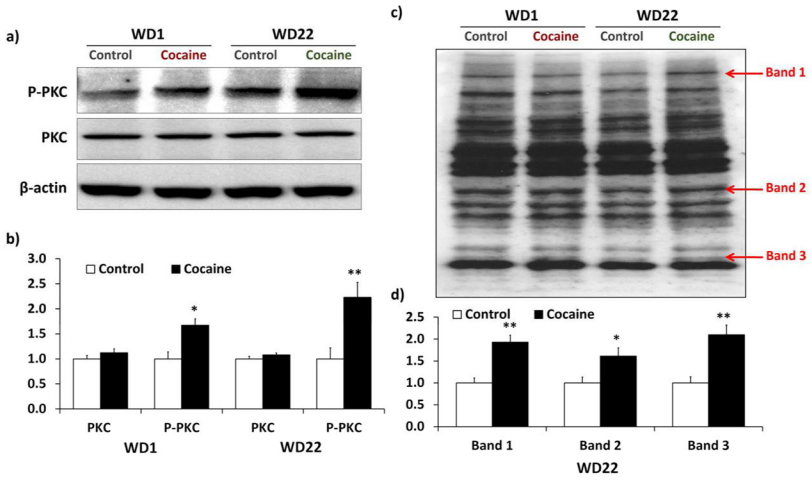

Figure 4.

Western blot analysis of PKC expression and activity. a) Representative images from Western blot images of PKC and p-PKC in both WD1 and WD22; b) Quantitative analysis of PKC and p-PKC by densitometry; c) Western blot images of p-PKC substrates; three exemplary bands are shown by the red arrows; d) Quantitative analysis of the three p-PKC substrates bands in WD22 by densitometry. Together the results implicated elevated phosphorylation and activity of PKC with long-term cocaine withdrawal.

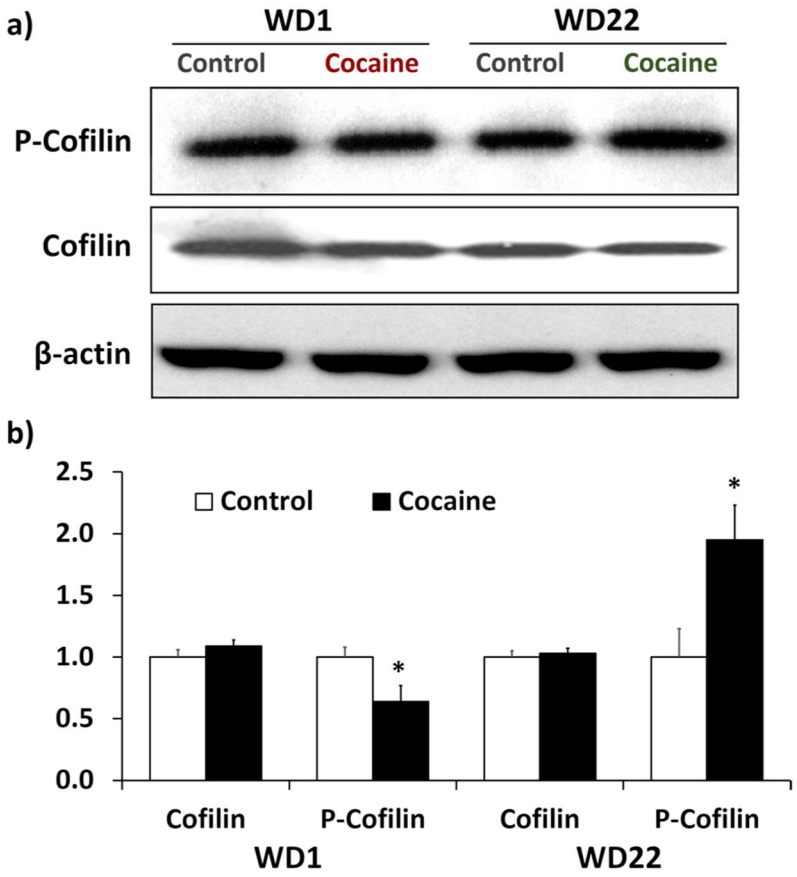

Figure 5.

Western blot analysis of cofilin-1 expression and activity. a) Western blot images in both WD1 and WD22; b) Quantitative analysis of Western blots by densitometry. Opposite trends of cofilin-1 phosphorylation were observed with 1d and 22d cocaine withdrawal.

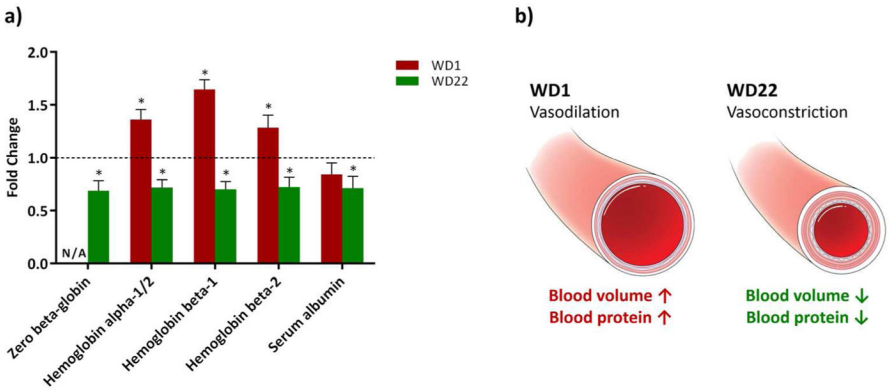

Figure 6.

Significantly decreased levels of five RBC/plasma proteins with long-term cocaine withdrawal. a) Fold changes of five selected RBC/plasma proteins quantified in the proteomic study. The dashed line represents the baseline level of the protein, and statistical significance ($p \leq 0.05$) between experimental and control groups is denoted with an asterisk. b) A graphic illustration of the mechanism underlying altered levels of blood proteins during chronic cocaine use and cocaine withdrawal.

Table 1

List of significantly-altered proteins belonging to functional categories of high interest. Significantly up-regulated and down-regulated proteins are highlighted in red and blue, respectively.

Protein AC #	Protein Name	Ratio	WD1 Standard Deviation	p-value	Ratio	WD22 Standard Deviation	p-value
Glycolysis							
P04797	Glyceraldehyde-3-phosphate dehydrogenase				1.02	0.04	>0.05
P04642	L-lactate dehydrogenase A chain				1.01	0.06	>0.05
P05065	Fructose-bisphosphate aldolase A				0.982	0.04	>0.05
Tricarboxylic Acid Cycle							
Q920L2	Succinate dehydrogenase [ubiquinone] flavoprotein subunit				1.02	0.07	>0.05
Q68FX0	Isocitrate dehydrogenase [NAD] subunit beta, mitochondrial				1.05	0.07	<0.05
Q5BJZ3	Nicotinamide nucleotide transhydrogenase				1.02	0.2	>0.05
Oxidative Phosphorylation1							
P19234	NADH dehydrogenase [ubiquinone] flavoprotein 2				1.08	0.08	>0.05
Q641Y2	NADH dehydrogenase [ubiquinone] iron-sulfur protein 2				1.07	0.1	>0.05
G3V6D3	ATP synthase subunit beta				1.05	0.08	>0.05
Q561S0	NADH dehydrogenase [ubiquinone] 1 alpha subcomplex subunit 10				1.03	0.08	>0.05
Stress Response							
P63018	Heat shock cognate 71 kDa protein				1.03	0.03	<0.05
P48721	Stress-70 protein, mitochondrial						
O88600	Heat shock 70 kDa protein 4				1.04	0.03	<0.01
Q66HA8	Heat shock protein 105 kDa				1.08	0.1	>0.05
Neurotransmitter Metabolism							
P23977	Sodium-dependent dopamine transporter				1.23	0.3	>0.05
P50554	4-aminobutyrate aminotransferase, mitochondrial				1.11	0.1	<0.05
P10860	Glutamate dehydrogenase 1, mitochondrial				1.03	0.07	>0.05
P00507	Aspartate aminotransferase, mitochondrial				1.04	0.04	>0.05
P13221	Aspartate aminotransferase, cytoplasmic				1.08	0.2	>0.05
Cell Adhesion							

Protein AC #	Protein Name	Ratio	WD1 Standard Deviation	p-value	Ratio	WD22 Standard Deviation	p-value
A0A096MJE6	Tenascin-R				0.914	0.1	>0.05
P31977	Ezrin				0.870	0.1	>0.05
RBC/Plasma							
Q63011	Zero beta globin						
P02091	Hemoglobin subunit beta-1						
P11517	Hemoglobin subunit beta-2						
P01946	Hemoglobin subunit alpha-1/2						
P02770	Serum albumin	0.840	0.1	>0.05			
Regulation of Axonogenesis							
P07936	Neuromodulin				1.02	0.1	>0.05
P02688	Myelin basic protein						
Anti-Oxidant Responses							
P07895	Superoxide dismutase [Mn], mitochondrial				1.01	0.2	>0.05
P27139	Carbonic anhydrase 2	0.905	0.2	>0.05			
P04906	Glutathione S-transferase P	1.02	0.2	>0.05			
Intracellular Transport							
F1LRK0	Clathrin coat assembly protein AP180						
Q9WUW2	Vesicle associated membrane protein 2B				1.08	0.08	<0.05
G3V733	Synapsin-2				1.06	0.1	>0.05
Q5FVI6	V-type proton ATPase subunit C 1				1.00	0.1	>0.05
Q5M7T6	ATPase, H+ transporting, lysosomal				0.966	0.08	>0.05
P61107	Ras-related protein Rab-14				1.07	0.06	<0.05
P41542	General vesicular transport factor p115				0.985	0.1	>0.05
G Protein Signaling							
Q9R080	G-protein-signaling modulator 1 (Activator of G-protein signaling 3)						
G3V8E8	Guanine nucleotide-binding protein G(olf) subunit alpha				1.04	0.2	>0.05
P43425	Guanine nucleotide-binding protein G(I)/G(S)/G(O) subunit gamma-7				1.23	0.2	>0.05
P10824	Guanine nucleotide-binding protein G(i) subunit alpha-1				0.966	0.1	>0.05

Protein AC #	Protein Name	Ratio	WD1 Standard Deviation	p-value	Ratio	WD22 Standard Deviation	p-value
cAMP Signaling							
Q08163	Adenylyl cyclase-associated protein 1 (CAP 1)				1.07	0.1	>0.05
Q04400/G3V9G1	Adenylate cyclase type 5 (EC 4.6.1.1) (ATP pyrophosphate-lyase 5) (Adenylate cyclase type V) (Adenylyl cyclase 5)						
P12369	cAMP-dependent protein kinase type II-beta regulatory subunit				1.15	0.1	<0.05
Calcium Signaling							
Q9ESB4	Neuronal calcium binding protein NECAB2						
P07171	Calbindin				1.17	0.2	<0.05
Q01066	Calcium/calmodulin-dependent 3′,5′-cyclic nucleotide phosphodiesterase 1B				1.25	0.2	>0.05
P11275	Calcium/calmodulin-dependent protein kinase type II subunit alpha (CaM kinase II subunit alpha) (CaMK-II subunit alpha) (EC 2.7.11.17)				0.973	0.04	>0.05
C7E1V2/P29994	Inositol 1,4,5-trisphosphate receptor type 1				1.16	0.6	>0.05
P47728	Calretinin						
Phosphatase							
Q68G16	Serine/threonine-protein phosphatase (EC 3.1.3.16)				0.943	0.08	>0.05
P63329	Serine/threonine-protein phosphatase 2B catalytic subunit alpha				1.04	0.07	>0.05
P63331	Serine/threonine-protein phosphatase 2A catalytic subunit alpha						
Q8VD52	Pyridoxal phosphate phosphatase				1.10	0.2	>0.05
F1M978	Inositol monophosphatase 1				0.938	0.08	>0.05
P50411	Protein phosphatase inhibitor 2 (IPP-2)				1.19	0.1	<0.05
Cytoskeleton-Actin Filaments							
P45592	Cofilin-1						
Q91Y81	Septin-2				1.04	0.2	>0.05
Q6T487	Brain-specific alpha actinin 1				1.06	0.09	>0.05
Q4V7C7	Actin-related protein 3 (Actin-like protein 3)				1.09	0.09	>0.05
O35867	Neurabin-1				1.06	0.2	>0.05
F1LNB2	Phosphatase and actin regulator				1.16	0.2	>0.05
Cytoskeleton-Intermediate Filaments							
F1LRZ7	Neurofilament heavy polypeptide				0.975	0.2	>0.05
P19527	Neurofilament light polypeptide				0.955	0.2	>0.05

Protein AC #	Protein Name	Ratio	WD1 Standard Deviation	p-value	Ratio	WD22 Standard Deviation	p-value
P12839	Neurofilament medium polypeptide				0.952	0.1	>0.05
P47819	Glial fibrillary acidic protein				0.846	0.2	>0.05
Cytoskeleton-Microtubules							
O35303	Dynamin-1-like protein				1.00	0.08	>0.05
Q03555	Gephyrin				1.09	0.08	<0.05
Q9JHU0	Dihydropyrimidinase-related protein 5				1.06	0.05	>0.05
P13668	Stathmin	0.90	0.3	>0.05			